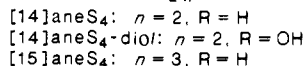
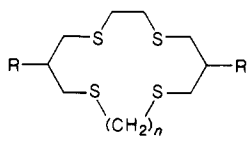


the stable conformers of Cu^{II}L and Cu^IL, respectively, and Q and P represent metastable conformers whose geometries more closely approximate the stable form of the other oxidation state.

Square schemes of the type shown in Scheme I have been postulated by Bond,⁸ Rieke,⁹ Geiger,¹⁰ and Walton¹¹ to explain the electrochemical behavior of a variety of systems, most of which involve cis-trans isomerization. Evans,¹² Bard,¹³ Taube,¹⁴ and Collins¹⁵ have reported electrochemical studies on other systems that appear to involve structural reorganization for either the oxidized or reduced species—but not both.

Laviron and Roullier¹⁶ have presented a generalized theoretical treatment for the type of electron-transfer scheme represented in Scheme I in which the stable species are located at diagonal corners of the square (i.e., species O and R) as is proposed for our system. In their presentation, they simulated the cyclic voltammetric curves that should be exhibited for different relative rate constant values. However, in analyzing the theoretical behavior of such systems, they treated only thin-layer solutions and included sweep rates differing by 12 orders of magnitude—a range of conditions impossible to achieve experimentally by cyclic voltammetry.¹⁷

We have now examined in greater detail the cyclic voltammetric behavior of Cu^{II/I}([14]aneS₄) and related systems [including, in particular, the copper complexes formed with 3,6,10,13-tetra-thiacyclotetradecane-1,8-diol ([14]aneS₄-diol) and 1,4,8,12-tet-



rathicyclopentadecane ([15]aneS₄)).¹⁸ By varying the temperature, we have attempted to demonstrate that the Cu^{II/I}([14]aneS₄) system mimics nearly all of the behavior predicted by Laviron and Roullier for a system in which one of the oxidant species (designated as Q in Scheme I) is extremely unstable. The resulting interpretation yields a unified explanation of electron transfer in Cu(II)/Cu(I) systems which appears to be consistent

with all known studies on both copper proteins and low molecular weight copper complexes.

Experimental Section

The electrochemical instrumentation used to obtain all cyclic voltammograms consisted of a Princeton Applied Research (PAR) Model 175 universal programmer, a PAR Model 173 potentiostat equipped with a Model 179 digital coulometer, a current-to-voltage converter, and an interfaced minicomputer.

For the first peak on any forward scan, the peak current was measured as the absolute difference between the peak current value and the decaying current base line obtained by holding the potential constant at the foot of the peak. The peak current for the first peak on a return scan was corrected by using, as a base line, the current obtained when the potential was held at the switching potential value. A second peak on the forward or reverse scan was measured as the absolute current corrected for the decaying current base line of the first peak. In all cases, the base line was obtained by recording the time-dependent current on a second voltammogram when the scan was stopped at the foot of the peak or at the switching potential.¹⁹

Low concentrations of the electroactive species (typically ≤0.5 mM) were used in cyclic voltammetric measurements in order to minimize the effect of ohmic potential losses.²⁰ The experimental curves, however, contain an observable amount of charging current.¹⁹ The reported potentials were measured against the saturated sodium chloride calomel reference electrode (SSCE, E⁰ = 0.247 V vs NHE)²¹ and were not corrected for junction potentials. Uncompensated resistance (R_u) in the voltammetric cell was not electronically compensated, because oscillations were detected when the positive feedback option was selected. It was observed that the separation between peak potentials yielded identical values with or without compensation of the solution resistance.

The auxiliary electrode consisted of a platinum coil. Glassy carbon press-fitted onto a Kel-F shroud (Bioanalytical Systems) was the working electrode used for most of the work described in this paper. The pretreatment for this electrode was based on the method recommended by Rusling and co-workers.²² For a few experiments a platinum button electrode was utilized.

Temperature control at ≥5 °C was maintained by circulating the fluid from a temperature bath through a jacket surrounding the covered cell. Lower temperatures were attained by immersing the cell into a sodium chloride-crushed ice mixture (T = 0 ± 1 °C), a dry ice-carbon tetrachloride bath (T = -23 ± 1 °C) or a dry ice-acetone bath (T = -77 ± 2 °C). The electrochemical experiments were performed under nonisothermal conditions²³ since the temperature of the reference electrode was not controlled.

The test solutions were prepared by dissolving recrystallized copper perchlorate and the macrocyclic ligand in distilled, deionized water of conductivity grade and, where applicable, reagent-grade methanol. Prior to use, these solutions were deoxygenated for at least 20 min with ultra-high-purity nitrogen. Copper(I) complex solutions were prepared by controlled potential electrolysis of the corresponding copper(II) solutions using a large platinum gauze electrode. Perchloric acid was the supporting electrolyte used in all electrochemical studies on the copper-polythiaether complexes.

Potentiostatic Measurements. Independent potentiostatic measurements of the E_{1/2} values were made by reducing Cu^{II}L solutions in a stepwise fashion while continuously flowing the solution through a spectrophotometric cell inserted in a Perkin-Elmer Lambda 3B double-beam scanning spectrophotometer equipped with a Model 3600 data station and a Model 660 printer. For these measurements, the potential was held constant until the current decayed to the background level (≈20–30 min) prior to scanning the UV-visible spectrum.²⁴ This process was repeated at 20-mV intervals bracketing the approximate formal potential value of the redox species of interest as located by slow scan

(8) (a) Wimmer, F. L.; Snow, M. R.; Bond, A. M. *Inorg. Chem.* **1974**, *13*, 1617–1623. (b) Bond, A. M.; Colton, R.; Jackowski, J. J. *Inorg. Chem.* **1975**, *14*, 274–278. (c) Bond, A. M.; Grabaric, B. S.; Jackowski, J. J. *Inorg. Chem.* **1978**, *17*, 2153–2157. (d) Bond, A. M.; Darensbourg, D. J.; Mocolin, E.; Stewart, B. J. *J. Am. Chem. Soc.* **1981**, *103*, 6827–6832. (e) Bond, A. M.; Oldham, K. B. *J. Phys. Chem.* **1983**, *87*, 2492–2502. (f) Bond, A. M.; Oldham, K. B. *J. Phys. Chem.* **1985**, *89*, 3739–3747.

(9) (a) Rieke, R. D.; Kojima, H.; Ofele, K. J. *J. Am. Chem. Soc.* **1976**, *98*, 6735–6737. (b) *Ibid.* *Angew. Chem., Int. Ed. Engl.* **1980**, *19*, 538–540. (c) Rieke, R. D.; Henry, W. P.; Arney, J. S. *Inorg. Chem.* **1987**, *26*, 420–427.

(10) Moraczewski, J.; Geiger, W. E. *J. Am. Chem. Soc.* **1979**, *101*, 3407–3408.

(11) Conner, K. A.; Walton, R. A. *Inorg. Chem.* **1986**, *25*, 4422–4430.

(12) (a) Nelsen, S. F.; Echegoyen, L.; Evans, D. H. *J. Am. Chem. Soc.* **1975**, *97*, 3530–3533. (b) Nelsen, S. F.; Echegoyen, L.; Clennan, E. L.; Evans, D. H.; Corrigan, D. A. *J. Am. Chem. Soc.* **1977**, *99*, 1130–1134. (c) Nelsen, S. F.; Clennan, E. L.; Evans, D. H. *J. Am. Chem. Soc.* **1978**, *100*, 4012–4019. (d) Olsen, B. A.; Evans, D. E. *J. Am. Chem. Soc.* **1981**, *103*, 839–843. (e) Evans, D. H.; O'Connell, K. M. In *Electroanalytical Chemistry*; Lippard, S. J., Ed.; Wiley: New York, 1985; Vol. 33, pp 275–352.

(13) (a) Gaudiello, J. G.; Wright, T. C.; Jones, R. A.; Bard, A. J. *J. Am. Chem. Soc.* **1985**, *107*, 888–897. (b) Moulton, R.; Weidman, T. W.; Vollhardt, K. P. C.; Bard, A. J. *Inorg. Chem.* **1986**, *25*, 1846–1851.

(14) Ilan, Y.; Taube, H. *Inorg. Chem.* **1983**, *22*, 1655–1664.

(15) (a) Anson, F. C.; Collins, T. J.; Gipson, S. L.; Keech, J. T.; Kraft, T. E.; Peake, G. T. *J. Am. Chem. Soc.* **1986**, *108*, 6593–6605. (b) Collins, T. J.; Keech, J. T. *J. Am. Chem. Soc.* **1988**, *110*, 1162–1167.

(16) Laviron, E.; Roullier, L. *J. Electroanal. Chem.* **1985**, *186*, 1–15.

(17) In a subsequent paper, in which Laviron and Roullier applied the theory to a real system, all measurements were carried out at 60 °C in order to determine all the equilibrium and rate constants associated with Scheme I: Vallat, A.; Person, M.; Roullier, L.; Laviron, E. *Inorg. Chem.* **1987**, *26*, 332–335.

(18) For the smaller macrocyclic polythiaethers, [12]- and [13]aneS₄, the Cu(I) complexes were not sufficiently soluble to permit a thorough study of their electrochemical behavior.

(19) The procedure utilized for base-line correction eliminates the contribution of the faradaic current produced by an earlier peak but does not correct for charging current. In the case of a peak on the return scan, few other means exist for establishing a reliable base line. The procedure described permits a reasonable method for comparing the heights of peaks on the forward and return scan (i.e., *i*_{pa}/*i*_{pc}) since the charging current contribution to the various peaks should be nearly constant in any single voltammogram.

(20) Nicholson, R. S. *Anal. Chem.* **1965**, *37*, 1351–1355.

(21) Meites, L.; Zuman, P.; Narayanan, A.; Rupp, E. B. *Handbook Series in Inorganic Electrochemistry*; CRC: Boca Raton, FL, 1983.

(22) Kamau, G. N.; Willis, W. S.; Rusling, J. F. *Anal. Chem.* **1985**, *57*, 545–551.

(23) Yee, E. L.; Cave, R. J.; Guyer, K. L.; Tyma, P. D.; Weaver, M. J. *J. Am. Chem. Soc.* **1979**, *101*, 1131–1137.

(24) Betsu, S. R.; Klapper, M. H.; Anderson, L. B. *J. Am. Chem. Soc.* **1972**, *94*, 8197–8204.

Table I. Specific Peak Potential Values and Peak Current Ratios for $\text{Cu}^{\text{II}}/([\text{14}] \text{aneS}_4)$ in 80% MeOH, 0.1 M HClO_4 , at a Glassy Carbon Electrode: $C_{\text{Cu}} = 4.98 \text{ mM}$, $C_{\text{L}} = 0.50 \text{ mM}$, $T = +25 \text{ }^\circ\text{C}$

v , V s^{-1}	E_{pl} , V	$\Delta E_{\text{p(II-I)}}$, mV	$E_{1/2}$, V	$i_{\text{pII}}/i_{\text{pI}}$	E_{pIII} , V	$\Delta E_{\text{p(III-I)}}$, mV
$\text{Cu}^{\text{II}}([\text{14}] \text{aneS}_4)$						
0.010	0.40	63	0.43	1.00		
0.021	0.40	64	0.44	1.00		
0.051	0.40	67	0.44	0.96		
0.102	0.40	73	0.44	0.94		
0.202	0.39	86	0.44	0.90		
0.505	0.39	101	0.44	0.86	0.62	230
0.992	0.38	114	0.44	0.86	0.62	242
1.982	0.38	135	0.45	0.87	0.64	261
4.961	0.36	177	0.45	0.83	0.66	305
9.933	0.36	160	0.44	0.90	0.67	317
$\text{Cu}^{\text{I}}([\text{14}] \text{aneS}_4)$						
0.010	0.41	66	0.44	1.02		
0.020	0.41	71	0.44	0.95		
0.050	0.41	78	0.44	0.90		
0.100	0.41	81	0.45	0.91		
0.202	0.40	93	0.45	0.89		
0.504	0.39	104	0.44	0.71	0.64	253
0.986	0.38	116	0.44	0.75	0.65	274
1.976	0.38	129	0.44	0.66	0.66	278
4.939	0.37				0.68	314

cyclic voltammetry. In view of the limited stability of the $\text{Cu}^{\text{II}}\text{L}$ species,²⁵ a large excess of $\text{Cu}(\text{II})$ ion was added to these solutions to insure that $\text{Cu}^{\text{II}}\text{L}$ was fully formed at all times.

Results

Voltammetric Behavior of $\text{Cu}^{\text{II}}/([\text{14}] \text{aneS}_4)$ in Aqueous Solution.

Cyclic voltammograms of aqueous solutions containing $\text{Cu}^{\text{II}}\text{L}$ (where L represents $[\text{14}] \text{aneS}_4$) show essentially reversible behavior under slow-scan conditions at $25 \text{ }^\circ\text{C}$ ($\Delta E_{\text{p}} = 65 \text{ mV}$ at $v = 0.02 \text{ V s}^{-1}$; $i_{\text{pa}}/i_{\text{pc}} = 1.0$ at $v \leq 1 \text{ V s}^{-1}$) with an $E_{1/2}$ value of $\approx 0.35 \text{ V}$ (vs SSCE). However, as the scan rate is increased above 100 V s^{-1} , a second anodic peak begins to develop at $\approx 0.60 \text{ V}$ and grows at the expense of the original anodic peak. Consistent behavior is observed for solutions containing $\text{Cu}^{\text{I}}\text{L}$.

By lowering the temperature to $5 \text{ }^\circ\text{C}$, the appearance of the more positive anodic peak is more readily observed, although this peak still does not become obvious until the scan rate reaches at least 50 V s^{-1} . Unfortunately, with the electrodes used in this work, cyclic voltammograms obtained at scan rates above 10 V s^{-1} could not be analyzed quantitatively. However, the trend in peak behavior with temperature implies the involvement of a chemical reaction for which the pertinent kinetic processes are slowed at the lower temperature.

The foregoing observations suggested that the use of even lower temperatures might make it possible to analyze the behavior of the two anodic peaks and, in addition, might reveal electrochemical features that would otherwise require inaccessibly rapid scan rates. Such an approach has been supported by Van Duyne and Reilley,²⁶ who have noted that, by decreasing the rate constants for the chemical processes, voltammograms at lowered temperatures can be considered qualitatively equivalent to the behavior that would be observed at more rapid scan rates at $25 \text{ }^\circ\text{C}$.

Recognizing that significantly lower temperatures were not feasible in aqueous solution, we selected 80% methanol (w/w) as the solvent matrix.²⁷ It was also noted that, even at $25 \text{ }^\circ\text{C}$, the more positive anodic peak could be observed at considerably slower

(25) (a) Sokol, L. S. W. L.; Ochrymowycz, L. A.; Rorabacher, D. B. *Inorg. Chem.* **1981**, *20*, 3189–3195. (b) Young, I. R.; Ochrymowycz, L. A.; Rorabacher, D. B. *Inorg. Chem.* **1986**, *25*, 2576–2582.

(26) Van Duyne, R. P.; Reilley, C. N. *Anal. Chem.* **1972**, *44*, 142–152; *Ibid.* 153–158 (see, e.g., p 155); *Ibid.* 158–169.

(27) Previous electrochemical studies and complex formation and dissociation kinetic studies on the copper-polythiaether complexes in 80% methanol have demonstrated that the behavior of these systems is qualitatively similar in both water and 80% methanol: (a) Dockal, E. R.; Jones, T. E.; Sokol, W. F.; Engerer, R. J.; Rorabacher, D. B.; Ochrymowycz, L. A. *J. Am. Chem. Soc.* **1976**, *98*, 4322–4324. (b) Diaddario, L. L.; Zimmer, L. L.; Jones, T. E.; Sokol, L. S. W. L.; Cruz, R. B.; Yee, E. L.; Ochrymowycz, L. A.; Rorabacher, D. B. *J. Am. Chem. Soc.* **1979**, *101*, 3511–3520.

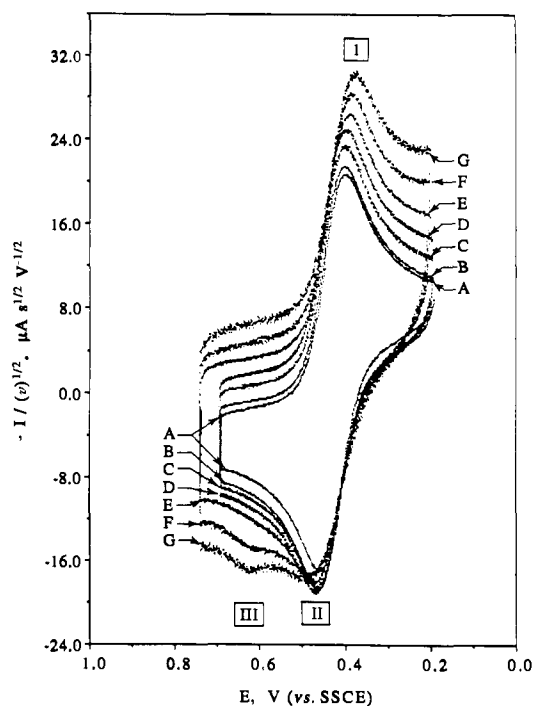


Figure 1. Effect of scan rate on cyclic voltammograms of $\text{Cu}^{\text{II}}([\text{14}] \text{aneS}_4)$ in 80% MeOH, 0.1 M HClO_4 , at a glassy carbon electrode showing the development of peak III: scan rates, (A) 0.010, (B) 0.020, (C) 0.050, (D) 0.100, (E) 0.200, (F) 0.500, (G) 1.000 V s^{-1} ; $T = +25 \text{ }^\circ\text{C}$.

scan rates in 80% methanol than in water.

Detailed Voltammetric Behavior of $\text{Cu}^{\text{II}}/([\text{14}] \text{aneS}_4)$ in 80% Methanol. When the potential was limited to the range from $+0.70$ to $+0.19 \text{ V}$, the series of cyclic voltammograms shown in Figure 1 was obtained at $25 \text{ }^\circ\text{C}$. The corresponding cyclic voltammetric data are listed in Table I. A single cathodic peak (I) is observed under all conditions. At slow scan rates, ($v < 0.050 \text{ V s}^{-1}$), a single anodic peak (II) is observed with the anodic-cathodic peak potential separation ($\Delta E_{\text{p}} = E_{\text{pII}} - E_{\text{pI}}$), the anodic to cathodic peak current ratio ($i_{\text{pII}}/i_{\text{pI}}$), and the cathodic half-peak width values ($E_{\text{p}} - E_{\text{p}/2}$) closely approximating those expected for a one-electron reversible electrode process. When the scan rate is increased, however, the peaks become more separated with a constant $E_{1/2}$ value. The $i_{\text{pII}}/i_{\text{pI}}$ values diminish due, primarily, to the decrease of peak II. Concomitantly, an additional oxidation peak (peak III), which grows at the expense of peak II, is detected at more positive potentials at scan rates as slow as 0.500 V s^{-1} (Figure 1). Identical behavior is observed for $\text{Cu}^{\text{I}}\text{L}$ solutions, thus confirming the chemical reversibility of the electrode process.²⁸ For the latter solutions, however, peak III becomes apparent at lower scan rates than observed for $\text{Cu}^{\text{II}}\text{L}$ solutions (0.100 V s^{-1} for $\text{Cu}^{\text{I}}\text{L}$ as compared to 0.500 V s^{-1} for $\text{Cu}^{\text{II}}\text{L}$). When the potential of $\text{Cu}^{\text{II}}\text{L}$ solutions is held at the switching potential, enhancement of peak III relative to peak II is noted.

An analogous behavioral pattern is observed with $\text{Cu}^{\text{II}}\text{L}$ at a platinum electrode. The half-wave potential values, however, remain scan rate independent and essentially equal to $+0.44 \text{ V}$ at both electrodes (i.e., platinum and glassy carbon).

To assess the possible contribution of adsorption, cyclic voltammetry was conducted in solutions with $\text{Cu}^{\text{I}}\text{L}$ concentrations ranging from 4.6×10^{-4} to $2.1 \times 10^{-5} \text{ M}$ with the ionic strength maintained at 0.1 M with HClO_4 . The ratio of peak III to peak II is independent of $\text{Cu}^{\text{I}}\text{L}$ concentration. Furthermore, no shift of peak III is observed nor does peak III become symmetrical as the scan rate is increased or the concentration is decreased.

(28) (a) Bond, A. M.; Colton, R.; Kevekordes, J. E. *Inorg. Chem.* **1986**, *25*, 749–756. (b) Bodini, M. E.; Willis, L. A.; Riechel, T. L.; Sawyer, D. T. *Inorg. Chem.* **1976**, *15*, 1538–1543. (c) Bond, A. M.; Grabaric, B. S.; Grabaric, Z. *Inorg. Chem.* **1978**, *17*, 1013–1018.

Table II. Peak Potential Values as a Function of Scan Rate for $\text{Cu}^{\text{II}}/([\text{14}] \text{aneS}_4)$ in 80% MeOH, 0.1 M HClO_4 , at a Glassy Carbon Electrode: $C_{\text{Cu}} = 0.689 \text{ mM}$, $C_{\text{L}} = 0.700 \text{ mM}$, Variable Temperature

v , V s^{-1}	E_{pl} , V	E_{plI} , V	E_{plII} , V	$\Delta E_{\text{p(I-II)}}$, mV	$E_{1/2(\text{I/II})}$, V
$\text{Cu}^{\text{II}}([\text{14}] \text{aneS}_4)$					
$T = +25 \text{ }^\circ\text{C}$					
0.050	0.38	0.46		80	0.42
0.200	0.38	0.47		91	0.42
1.000	0.38	0.48	0.60	101	0.43
5.000	0.35	0.52	0.67	171	0.44
$T = 0 \text{ }^\circ\text{C}$					
0.050	0.37	0.45		78	0.41
0.200	0.37	0.46	0.60	95	0.42
1.000	0.36	0.48	0.64	126	0.42
5.000	0.33	0.50	0.69	168	0.41
$T = -23 \text{ }^\circ\text{C}$					
0.050	0.37	0.47	0.63	98	0.42
0.200	0.35	0.46	0.65	107	0.40
1.000	0.33	0.49	0.67	163	0.41
5.000	0.28	0.48	0.72	199	0.38
$T = -77 \text{ }^\circ\text{C}$					
0.050	0.29	0.49	0.66	210	0.39
0.200	0.28	0.47	0.67	192	0.37
1.000	0.22	0.52	0.70	306	0.37
5.000	0.09	0.61		526	0.35
$\text{Cu}^{\text{I}}([\text{14}] \text{aneS}_4)$					
$T = +25 \text{ }^\circ\text{C}$					
0.050	0.40	0.49	0.64	83	0.45
0.200	0.40	0.50	0.65	99	0.45
1.000	0.39	0.51	0.68	120	0.45
5.000	0.38	0.49	0.73	110	0.44
$T = 0 \text{ }^\circ\text{C}$					
0.050	0.39	0.49	0.64	76	0.44
0.200	0.39	0.54	0.65	150	0.47
1.000	0.37	0.49	0.69	123	0.43
5.000	0.33		0.74		
$T = -23 \text{ }^\circ\text{C}$					
0.050	0.37		0.65		
0.200	0.34		0.70		
1.000	0.32		0.71		
5.000	0.29		0.78		
$T = -77 \text{ }^\circ\text{C}$					
0.050	0.29		0.68		
0.200	0.28		0.71		
1.000	0.25		0.77		
5.000	0.12		0.96		

The effect of temperature on the cyclic voltammetric response of $\text{Cu}^{\text{II}}/[\text{14}] \text{aneS}_4$ was investigated in 80% MeOH, 0.1 M HClO_4 , at +25, 0, -23, and -77 $^\circ\text{C}$. The cyclic voltammetric data, as summarized in Table II, show interesting variations of peaks II and III with temperature, scan rate, and starting material (i.e., $\text{Cu}^{\text{I}}\text{L}$ or $\text{Cu}^{\text{II}}\text{L}$). Cyclic voltammograms of $\text{Cu}^{\text{II}}\text{L}$ at -23 $^\circ\text{C}$ as a function of scan rate show that peak III appears at slower scan rates at -23 $^\circ\text{C}$ (Figure 2) than at +25 $^\circ\text{C}$ (Figure 1). By lowering the temperature of a $\text{Cu}^{\text{II}}\text{L}$ solution to -77 $^\circ\text{C}$, peak II reappears at the expense of peak III (Figure 3). For $\text{Cu}^{\text{I}}\text{L}$ solutions, cyclic voltammograms at -23 $^\circ\text{C}$ show only peak III during the anodic sweep. Peak II does not reappear for such solutions even at -77 $^\circ\text{C}$ (Figure 4). However, peak II does appear in $\text{Cu}^{\text{I}}\text{L}$ solutions upon repeated cycling. In the cyclic voltammograms of $\text{Cu}^{\text{I}}\text{L}$ solutions at the lowest temperatures studied (i.e., -23 and -77 $^\circ\text{C}$), a new cathodic peak (IV) appears at ca. +0.65 V which increases slightly with increasing scan rate (Figure 4). The half-wave potential corresponding to peaks I and II is nearly independent of temperature or scan rate ranging from +0.42 V at 25 $^\circ\text{C}$ to +0.39 V at -77 $^\circ\text{C}$ (Table II, Figures 2-4). Careful current measurements of all peaks for $\text{Cu}^{\text{I}}\text{L}$ solutions show that the sum of the currents for peaks II and III reasonably approximates the sum for peaks I and IV at all temperatures examined (Table III).

Voltammetric Behavior of Related Systems. Voltammetric studies on a related copper-polythiaether complex, $\text{Cu}^{\text{II}}/([\text{14}]$ -

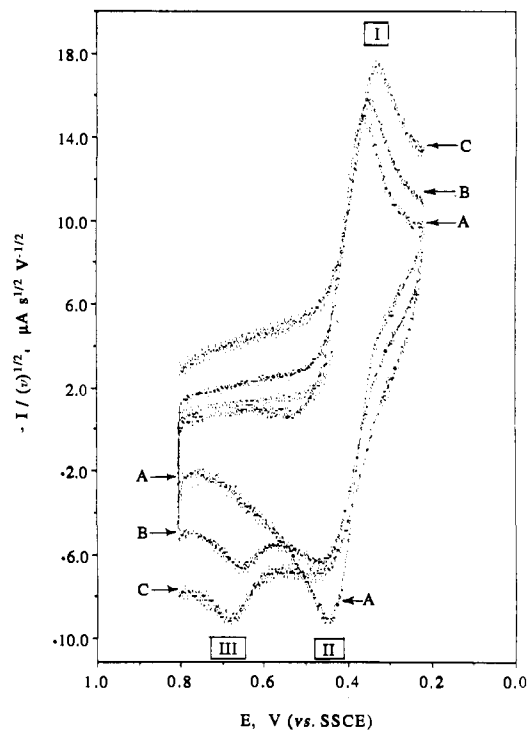


Figure 2. Effect of scan rate on low-temperature cyclic voltammograms of $\text{Cu}^{\text{II}}([\text{14}] \text{aneS}_4)$ in 80% MeOH, 0.1 M HClO_4 , at a glassy carbon electrode showing the development of peak III: scan rates, (A) 0.050, (B) 0.100, (C) 1.000 V s^{-1} ; $T = -23 \text{ }^\circ\text{C}$.

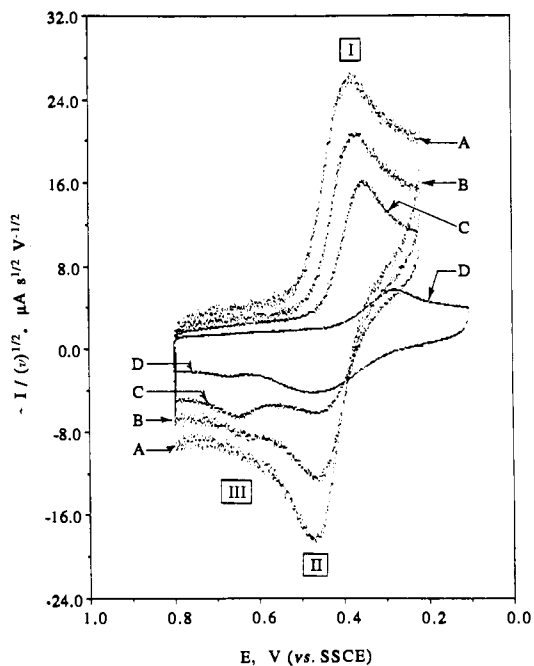


Figure 3. Effect of temperature on cyclic voltammograms of $\text{Cu}^{\text{II}}([\text{14}] \text{aneS}_4)$ in 80% MeOH, 0.1 M HClO_4 , at a glassy carbon electrode showing the development of peak III (curve C) followed by the subsequent redevelopment of peak II (curve D): scan rate, 0.200 V s^{-1} ; T , (A) +25, (B) 0, (C) -23, (D) -77 $^\circ\text{C}$.

ane S_4 -diol), yield similar behavior to that of $\text{Cu}^{\text{II}}/([\text{14}] \text{aneS}_4)$. By contrast, the behavior of the $\text{Cu}^{\text{II}}/([\text{15}] \text{aneS}_4)$ system is dramatically different from that for the 14-membered macrocyclic complexes. Under all temperature conditions and at all sweep rates, the system shows nearly completely reversible behavior with an $E_{1/2}$ value of 0.38 V (vs SSCE) in water and 0.57 V in 80% methanol ($\Delta E_{\text{p}} = 60 \text{ mV}$; $i_{\text{plI}}/i_{\text{pl}} = 1.0$ at $v = 0.02 \text{ V s}^{-1}$ in both solvents). Consistent results are obtained for $\text{Cu}^{\text{I}}\text{L}$ solutions. Controlled potential reductive electrolysis at +0.36 V yields $n = 0.98$.

Table III. Specific Peak Potential and Peak Current Values as a Function of Scan Rate for $\text{Cu}^{\text{I}}([\text{14}] \text{aneS}_4)$ in 80% MeOH, 1 M HClO_4 ,^a at a Glassy Carbon Electrode: $C_{\text{Cu}} = 99.6 \text{ mM}$, $C_{\text{L}} = 0.998 \text{ mM}$, Variable Temperature

ν , V s^{-1}	E_{pI} , V	E_{pII} , V	E_{pIII} , V	E_{pIV} , V	$E_{1/2(\text{I-II})}$, V	$E_{1/2(\text{IV-III})}$, V	i_{pI} , μA	i_{pII} , μA	i_{pIII} , μA	i_{pIV} , μA	$(i_{\text{pII}} + i_{\text{pIII}})/$ $(i_{\text{pI}} + i_{\text{pIV}})$
<i>T</i> = 0 °C											
0.020	0.29	0.40	0.56	0.44	0.34	0.50	-4.1	2.1	4.0	-1.7	1.05
0.050	0.29	0.38	0.56	0.43	0.34	0.49	-7.9	3.2	9.3	-2.8	1.17
0.100	0.27	0.38	0.59	0.45	0.33	0.52	-9.7	3.2	11.7	-4.5	1.05
0.987	0.26	0.40	0.59	0.47	0.33	0.53	-32.5	12.9	50.9	-20.0	1.22
<i>T</i> = -23 °C											
0.020	0.26	0.44	0.57	0.47	0.35	0.52	-3.0	0.9	4.1	-1.2	1.19
0.100	0.26	0.38	0.58	0.45	0.32	0.52	-7.2	1.8	10.6	-3.6	1.15
0.983	0.23		0.61	0.47		0.54	-22.6		43.4	-14.5	1.17
<i>T</i> = -77 °C											
0.020	0.21		0.60	0.47		0.53	-0.9		2.0	-0.5	1.4
0.101	0.21		0.62	0.44		0.53	-2.5		4.7	-1.5	1.18
1.006	0.19		0.66	0.47		0.56	-8.3		17.5	-7.7	1.09

^aNote that the higher concentration of HClO_4 used in this study causes a shift in the potential to lower values, presumably due to the stabilization of the $\text{Cu}^{\text{II}}\text{L}$ species (ref 25).

Table IV. Comparison of E^f Values from Potentiostatic Measurements and $E_{1/2}$ Values from Slow Scan Cyclic Voltammetric Measurements in H_2O and 80% MeOH, 0.1 M HClO_4 , $T = 25 \text{ }^\circ\text{C}$, at a Glassy Carbon Electrode (All Values in This Table are Referenced to Aqueous NHE)

redox couple	this work			ref 31
	$E^f(\text{H}_2\text{O})$, ^a V	$E_{1/2}(\text{H}_2\text{O})$, V	$E_{1/2}(80\% \text{ MeOH})$, V	$E_{1/2}(80\% \text{ MeOH})$, V
$\text{Cu}^{\text{II}}/([\text{14}] \text{aneS}_4)$	0.57–0.58	0.59–0.61	0.68–0.69	0.69
$\text{Cu}^{\text{II}}/([\text{14}] \text{aneS}_4\text{-diol})$ ^b		0.52–0.53	0.55–0.56	
$\text{Cu}^{\text{II}}/([\text{15}] \text{aneS}_4)$	0.65–0.68	0.63–0.65	0.81–0.82	0.79

^a E^f values were determined from spectral measurements at controlled potentials (see text). ^bThe [14]aneS₄-diol sample used for these measurements consisted primarily of the trans isomer with the cis isomer as a minor contaminant (cf: Pett, V. B.; Leggett, G. H.; Cooper, T. H.; Reed, P. R.; Situmang, D.; Ochrymowycz, L. A.; Rorabacher, D. B. *Inorg. Chem.* **1988**, *27*, 2164–2169).

Potentiostatic Determination of E^f . Spectra of aqueous solutions initially containing only $\text{Cu}^{\text{II}}\text{L}$ or $\text{Cu}^{\text{I}}\text{L}$ were run following a series of controlled potential electrolyses at several different potentials. The resultant absorbance (i.e., $\text{Cu}^{\text{II}}\text{L}$ concentration) vs potential plots yield apparent formal potentials for the $\text{Cu}(\text{II})/\text{Cu}(\text{I})$ redox couples under equilibrium conditions. These plots are linear with Nernstian slope for both the reduction of $\text{Cu}^{\text{II}}\text{L}$ and the oxidation of $\text{Cu}^{\text{I}}\text{L}$, and the E^f values obtained are identical within experimental error. These potentials agree closely with the slow scan $E_{1/2}$ values of the corresponding aqueous solutions (Table IV).

Discussion

General Behavior Predicted by the Square Scheme. The large difference in the coordination geometry normally found for $\text{Cu}(\text{II})$ and $\text{Cu}(\text{I})$ complexes with the same ligand requires that significant conformational change must accompany electron transfer in any $\text{Cu}^{\text{II}}\text{L}/\text{Cu}^{\text{I}}\text{L}$ system in which the coordination environment is not rigidly controlled. These geometric alterations may appear to be concerted or sequential with the electron-transfer step depending upon (i) the relative rate constants for such conformational changes in the absence of electron transfer and (ii) the time resolution of the experimental reference used.²⁹

For the systems reported here, the agreement between the $E_{1/2}$ values obtained from slow scan cyclic voltammograms and the E^f values obtained from the potentiostatic measurements indicate that the slow scan voltammograms represent equilibrium conditions. Moreover, for the current work, the observed similarities of the peak heights and peak positions on different electrodes and their essentially linear dependence on concentration and on the square root of the sweep rate strongly support the conclusion that both anodic peaks are mass-transfer controlled and that adsorption plays no significant role.³⁰ Thus, the deviant behavior noted for the $\text{Cu}^{\text{II}}/([\text{14}] \text{aneS}_4)$ system at faster scan rates and/or lower temperatures is due to chemical processes rather

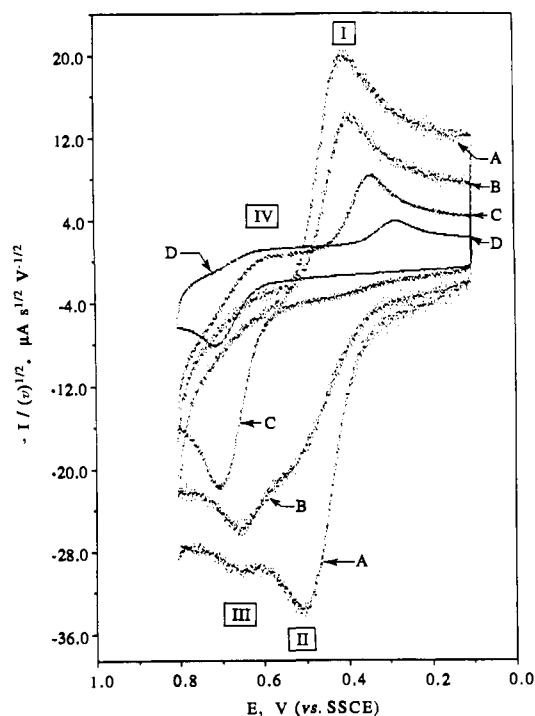


Figure 4. Effect of temperature on cyclic voltammograms of $\text{Cu}^{\text{I}}([\text{14}] \text{aneS}_4)$ in 80% MeOH, 0.1 M HClO_4 , at a glassy carbon electrode showing the development of peak III at the expense of peak II and the slight emergence of peak IV: scan rate, 0.200 V s^{-1} ; *T*, (A) +25, (B) 0, (C) -23, (D) -77 °C.

than to the electron-transfer step.

To facilitate the interpretation of our experimental electrochemical data, we define the following terms:^{16,31}

$$K_{\text{OQ}} = [\text{Q}]/[\text{O}] = k_{\text{OQ}}/k_{\text{QO}} \quad (3)$$

$$K_{\text{PR}} = [\text{R}]/[\text{P}] = k_{\text{PR}}/k_{\text{RP}} \quad (4)$$

$$I_{\text{OQ}} = k_{\text{OQ}} + k_{\text{QO}} \quad (5)$$

(29) Geiger, W. E. *Prog. Inorg. Chem.* **1985**, *33*, 275–352.

(30) Adsorption should yield a symmetrical peak, which increases linearly with scan rate, as well as a corresponding cathodic peak: Wopschall, A. H.; Shain, I. *Anal. Chem.* **1967**, *39*, 1535–1542. Neither of these features is observed in this work.

$$l_{PR} = k_{PR} + k_{RP} \quad (6)$$

$$a = (n\mathcal{F}/RT)v \quad (7)$$

where k_{OQ} , k_{QO} , k_{PR} , and k_{RP} are defined by Scheme I, a is Nicholson and Shain's scan rate parameter,³¹ and v is the scan rate in $V s^{-1}$.

Assuming that Scheme I represents the mechanism for electron transfer for the copper-polythiaether complexes, only a single cathodic and a single anodic peak would be observed at slow scan rates ($l_{OQ} \gg a \ll l_{PR}$), thus allowing the complete equilibration of $O \rightleftharpoons Q$ and $P \rightleftharpoons R$. We propose that this is the prevailing set of conditions observed for the cyclic voltammograms of $Cu^{II/1}([15]aneS_4)$ under all conditions studied and for the $Cu^{II/1}([14]aneS_4)$ and $Cu^{II/1}([14]aneS_4\text{-diol})$ systems at slow sweep rates.

By contrast, at very fast scan rates ($l_{OQ} \ll a \gg l_{PR}$), separate peaks would appear in $Cu^I L$ solutions for the oxidation of P and R and in $Cu^{II} L$ solutions for the reduction of Q and O with the relative peak heights proportional to the equilibrium concentrations of each species. For intermediate scan rates (i.e., $l \approx a$), the relative heights of the individual peaks would be dependent on the l/a ratio and the equilibrium constants for $O \rightleftharpoons Q$ and $P \rightleftharpoons R$ (i.e., K_{OQ} and K_{PR}).

Interpretation of Specific Voltammetric Behavior. The failure to observe peak IV in $Cu^{II} L$ solutions at any scan rate implies either that Q and O are always in equilibrium (i.e., $k_{OQ} \gg a \ll k_{QO}$) or that too little Q is present initially to be observed ($K_{OQ} \ll 1$). Furthermore, the fact that peak IV does begin to emerge in $Cu^I L$ solutions but never becomes well developed at any scan rate utilized implies both that $k_{QO} \gg a$ and that $K_{OQ} \ll 1$. Since the latter conditions are consistent with both observations, we conclude that, for both $Cu^{II/1}([14]aneS_4)$ and its diol derivative, Q is a very unstable intermediate that converts rapidly to O relative to the scan rates attainable in this study.

For $Cu^I L$ solutions, the shape, the relative intensity, and the potential variation with scan rate of peak III is characteristic of an $E_{rev}C_{irr}$ type of mechanism; an irreversible electrode process for this type of mechanism would yield a shallower, broader peak. These features become obvious in the low-temperature cyclic voltammograms of the $Cu^I L$ species. In addition, the peak potential shift approximates that predicted for an $E_{rev}C_{irr}$ mechanism, i.e., a 30-mV shift for each 10-fold increase in scan rate (Table II).³¹

From the foregoing analysis, it is clear that peaks II and III are related by a chemical process and that peak II results from a CE mechanism in $Cu^I L$ solutions. In fact, for slow scan rates ($l_{PR} \gg a$), peak II represents the oxidation of equilibrated $P \rightleftharpoons R$ to $O \rightleftharpoons Q$. For $Cu^I L$ solutions at rapid scan rates ($l_{PR} \ll a$), peak II represents the direct oxidation of $P \rightarrow O$, and therefore, the relative heights of peaks II and III should represent the relative initial concentrations of P and R, respectively. Since peak II is barely observed under these conditions (Figure 4), it is obvious that species P is relatively unstable with respect to R (i.e., $K_{PR} \gg 1$).

The situation is somewhat more complex for $Cu^{II} L$ solutions since peak II now represents the return of an $E_{rev}C_{rev}$ mechanism. As the scan rate is increased in $Cu^{II} L$ solutions, peak II diminishes but does not disappear under conditions for which corresponding $Cu^I L$ solutions no longer give evidence of this peak.³² This situation can only result if k_{PR} and k_{RP} do not differ by more than

an order of magnitude or so (i.e., $K_{PR} \ll 10^2$). In fact, as the scan rate is increased even further for $Cu^{II} L$ solutions, peak II begins to increase again at the expense of peak III (Figure 3, curve D for $-77^\circ C$). Under these conditions, the P produced in peak I during the cathodic sweep has insufficient time to convert completely to R before being reoxidized (i.e., $a \gg k_{PR}$). This interpretation is confirmed by the observation that, upon pausing at the switching potential following the cathodic sweep in $Cu^{II} L$ solutions (under conditions in which both peaks II and III are observed), peak III increases again at the expense of peak II. Furthermore, pausing at a potential midway between peaks II and III in the return sweep causes peak III to disappear completely.

As has been noted, only peak I is generally observed during the cathodic sweep for both $Cu^{II} L$ and $Cu^I L$ solutions. This peak represents the reduction of equilibrated $O \rightleftharpoons Q$ to $P \rightleftharpoons R$. However, since $K_{OQ} \ll 1$, peak I may be interpreted to represent primarily $O \rightarrow P$. Thus, under all conditions other than the most rapid scan rates, the height of peak I is approximately equal to the sum of peaks II and III. When peak IV is observed to emerge in $Cu^I L$ solutions at very fast sweep rates (Figure 4), the sum of peaks I and IV is also approximately equal to the sum of peaks II and III (Table III).

Estimation of Microscopic Potentials, Rate Constants, and Equilibrium Constants. Based on the experimental data obtained, estimates of the individual rate constants and equilibrium constants can be generated. The equilibrium constants, in particular, can be estimated with reasonable accuracy by relating the two microscopic redox couples, E_A^0 and E_B^0 ,



to the thermodynamic potential for the overall equilibrated system, E_K^0 :



As shown by Laviron and Roullier,¹⁶ the microscopic potentials are related to E_K^0 by the equilibrium constants, K_{OQ} and K_{PR} , according to the relationships

$$E_A^0 = E_K^0 - (RT/n\mathcal{F}) \ln [(1 + K_{PR})/(1 + K_{OQ})] \quad (11)$$

$$E_B^0 = E_K^0 - (RT/n\mathcal{F}) \ln [(1 + K_{PR}^{-1})/(1 + K_{OQ}^{-1})] \quad (12)$$

The values of $E_K^0 \approx 0.44$ V in 80% methanol (vs SSCE at 25 $^\circ C$) and $E_K^0 \approx 0.35$ V in water have been well established for $Cu^{II/1}([14]aneS_4)$ from slow scan CV measurements and from controlled potential spectrophotometric measurements (Table IV). In a $Cu^I L$ solution, peak III emerges approximately 0.20–0.21 V more positive than peak II in both solvents at 25 $^\circ C$. (The position of the shoulder designated as peak IV is also consistent with a value of $E_B^0 \approx 0.63$ V in 80% methanol at all temperatures.) This indicates that $E_B^0 - E_K^0 \approx 0.20$ V in both cases. With this value, eq 12 yields $K_{OQ} \approx 4 \times 10^{-4}$ (assuming $K_{PR} \gg 1$). The values of the other rate constants and equilibrium constants in Scheme I (for 80% methanol) can be estimated for the $Cu^{II/1}([14]aneS_4)$ system from the dependence of the voltammetric peaks on the scan rate and other experimental parameters (see Supplementary Material) as follows: $E_A^0 < 0.35$ V; $k_{QO} > 2 \times 10^3 s^{-1}$, $k_{OQ} > 1 s^{-1}$, $10 < K_{PR} < 10^2$, $k_{PR} \approx 10^4 s^{-1}$, $k_{RP} \approx 10^3 s^{-1}$.

Simulated Cyclic Voltammetric Curves. The complexity of Scheme I precludes simple predictions of the detailed voltammetric behavior other than in extreme cases. To demonstrate the efficacy of the square mechanism to account for our observed electrochemical behavior, we have generated simulated cyclic voltammograms based upon this model³³ using a wide variety of values for the rate constants representing the various conformational interconversions. The simulated voltammograms shown in Figures 5 and 6 represent one such series of curves for hypothetical solutions of $Cu^{II} L$ and $Cu^I L$, respectively, in which k_{PR} , k_{RP} , and

(31) Nicholson, R. S.; Shain, I. *Anal. Chem.* **1964**, *36*, 706–723. Nicholson and Shain have noted that apparent $E_{rev}C_{irr}$ behavior does not require that the chemical reaction itself is irreversible, but may represent a situation involving a large equilibrium constant for the chemical reaction following the electron-transfer step. Moreover, in applying this analysis specifically to the square scheme, Laviron and Roullier¹⁶ have pointed out that, when $K_{OQ} \ll 1$ (as is evident from the absence of peak IV), the portion of the scheme involving $R \rightarrow Q$ (peak III) will behave as an $E_{rev}C_{irr}$ system. Thus, we conclude that the behavior of peak III is totally consistent with the square scheme under these conditions.

(32) For $Cu^I L$ solutions, however, the behavior upon making successive scans is similar to that for $Cu^{II} L$ solutions (i.e., peak II still appears at fast scan rates upon making successive sweeps). See Supplementary Material.

(33) Schroeder, R. R.; Robandt, P. V., to be published.

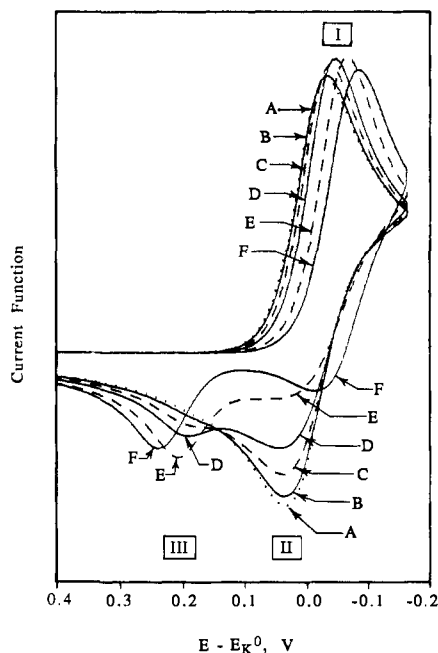


Figure 5. Simulated cyclic voltammograms for a $\text{Cu}^{\text{II}}\text{L}$ solution using $k_{\text{OQ}} = 10^1 \text{ s}^{-1}$, $k_{\text{QO}} = 10^5 \text{ s}^{-1}$, $k_{\text{PR}} = 10^4 \text{ s}^{-1}$, and $k_{\text{RP}} = 10^3 \text{ s}^{-1}$; scan rates, (A, ...) 0.010, (B, —) 0.10, (C, - -) 1.0, (D, —) 10, (E, - -) 100, (F, —) 1000 V s^{-1} . Potential values are normalized to E_{K}^0 .

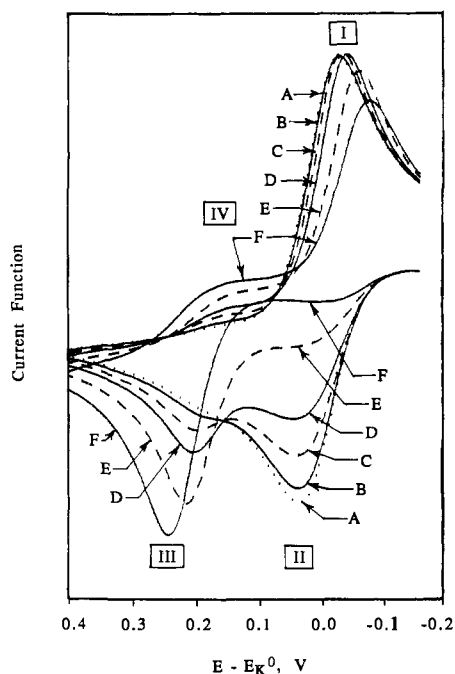
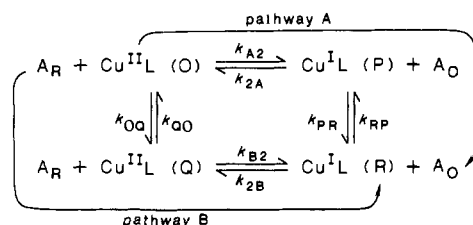


Figure 6. Simulated cyclic voltammograms for a $\text{Cu}^{\text{I}}\text{L}$ solution using $k_{\text{OQ}} = 10^1 \text{ s}^{-1}$, $k_{\text{QO}} = 10^5 \text{ s}^{-1}$, $k_{\text{PR}} = 10^4 \text{ s}^{-1}$, and $k_{\text{RP}} = 10^3 \text{ s}^{-1}$; scan rates, (A, ...) 0.010, (B, —) 0.10; (C, - -) 1.0, (D, —) 10, (E, - -) 100; (F, —) 1000 V s^{-1} . Potential values are normalized to E_{K}^0 .

k_{OQ} have been assigned values approximating those estimated from our experimental data, i.e., 10^4 s^{-1} , 10^3 s^{-1} , and 10^{-3} , respectively.³⁴ The appearance of these simulated voltammograms, covering a range of sweep rates from 0.010 to 1000 V s^{-1} , satisfactorily

(34) By varying the rate constants used in simulations the cyclic voltammograms, we have been able to establish that, in order to approximate our experimental curves, values of k_{PR} , k_{RP} , and k_{OQ} very close to our estimates are required. By contrast, the values of $k_{\text{OQ}} \approx 10^1 \text{ s}^{-1}$ and $k_{\text{QO}} \approx 10^5 \text{ s}^{-1}$ selected for use in these simulations (which are higher than our estimated lower limits) can be varied considerably without having a discernible effect on the simulated $\text{Cu}^{\text{II}}\text{L}$ voltammograms and, in $\text{Cu}^{\text{I}}\text{L}$ voltammograms, only the magnitude of peak IV is affected at very fast scan rates—as long as the ratio of $k_{\text{OQ}}/k_{\text{QO}}$ (i.e., K_{OQ}) is kept constant.)

Scheme II



reproduces the trends seen in our experimental curves for $\text{Cu}^{\text{II}}\text{L}([\text{14}] \text{aneS}_4)$ solutions, differing only by the effects of the residual charging current.

Correlation of Conformational Interconversion Kinetics to Structure. The origin of the difference in the apparent kinetics of conformational interconversion for the $[\text{14}] \text{aneS}_4$ and $[\text{15}] \text{aneS}_4$ systems may be inferred from the known crystal structures of the $\text{Cu}(\text{I})$ and $\text{Cu}(\text{II})$ complexes. Both $\text{Cu}(\text{II})$ complexes appear to adopt relatively strain-free tetragonal geometries in which the copper is coplanar with the four donor atoms.³⁵ (In the crystals studied, the axial sites were occupied by perchlorate ions, but these may be replaced by solvent molecules in solution.)

In the reduced complex, $\text{Cu}^{\text{I}}([\text{14}] \text{aneS}_4)$, the ligand appears to have difficulty in adapting to a tetrahedral coordination geometry. For the actual resolved crystal structure of $\text{Cu}^{\text{I}}([\text{14}] \text{aneS}_4)$, one of the $\text{Cu}-\text{S}$ bonds was found to be ruptured with the free sulfur then forming a coordinate bond to the next adjacent $\text{Cu}(\text{I})$ atom to generate a 3-1 coordination polymer.⁵ Experimental kinetic evidence shows that this species is not polymeric in solution,⁷ however, and we have previously inferred that, in the stable solvated species, the $\text{Cu}(\text{I})$ atom may be coordinated to three sulfur donor atoms and one solvent molecule. This could imply that the species R and P represent conformers in which the $\text{Cu}(\text{I})$ coordination sphere consists of OS_3 and S_4 , respectively. Alternatively, both the R and P species may have all four sulfur donor atoms coordinated with the ligand in two alternate conformations. This latter hypothesis is supported by the crystal structure for the closely related complex, $\text{Cu}^{\text{I}}([\text{14}] \text{aneNS}_3)$, in which all four donor atoms are found to be coordinated to the $\text{Cu}(\text{I})$ atom.³⁶ Moreover, the NMR spectrum of $\text{Cu}^{\text{I}}([\text{14}] \text{aneS}_4)$ indicates that all four sulfur donors are equivalent with two alternate forms of the complex interconverting slowly on the NMR time scale.³⁷

Although the structure of $\text{Cu}^{\text{I}}([\text{15}] \text{aneS}_4)$ has not been completely solved, X-ray crystallographic data indicate that this slightly larger ligand adopts a tetrahedral coordination geometry around the $\text{Cu}(\text{I})$ atom.³⁶ Thus, it is likely that two conformers of $\text{Cu}^{\text{I}}([\text{15}] \text{aneS}_4)$ could more rapidly interconvert than is the case for the corresponding conformers of $\text{Cu}^{\text{I}}([\text{14}] \text{aneS}_4)$.

Application to Cross-Exchange Reactions. When the proposed square scheme is modified to include heterogeneous electron-transfer cross reactions (Scheme II), the apparent discrepancies previously observed in the literature can now be understood. For systems in which O and R are the stable species and $K_{\text{PR}} \gg K_{\text{OQ}}^{-1}$ (i.e., P is relatively more stable than Q), pathway A may be presumed to predominate for reactions involving the reduction of $\text{Cu}^{\text{II}}\text{L}$ (including self-exchange reactions).^{7,37} Under the same conditions, however, cross reactions involving the oxidation of $\text{Cu}^{\text{I}}\text{L}$ may follow either pathway depending upon the reaction conditions. Thus, the rate expression for the oxidation of $\text{Cu}^{\text{I}}\text{L}$ may be written as (disregarding any back-reaction)⁷

$$-\frac{d[\text{Cu}^{\text{I}}\text{L}]}{dt} = \left(\frac{k_{2A}k_{\text{RP}}}{k_{2A}[\text{A}_\text{O}] + k_{\text{PR}}} + k_{2B} \right) [\text{R}][\text{A}_\text{O}] \quad (13)$$

(35) (a) Glick, M. D.; Gavel, D. P.; Diaddario, L. L.; Rorabacher, D. B. *Inorg. Chem.* **1976**, *15*, 1190-1193. (b) Pett, V. B.; Diaddario, L. L., Jr.; Dockal, E. R.; Corfield, P. W. R.; Ceccarelli, C.; Glick, M. D.; Ochrymowycz, L. A.; Rorabacher, D. B. *Inorg. Chem.* **1983**, *22*, 3661-3670.

(36) Heeg, M. J.; Bernardo, M. M.; Ochrymowycz, L. A.; Rorabacher, D. B., unpublished results.

(37) Vande Linde, A. M. Q. Ph.D. Dissertation, Wayne State University: Detroit, MI, 1988.

for which three limiting cases exist:

$$-(d[\text{Cu}^{\text{I}}\text{L}]/dt) = K_{\text{PR}}^{-1}k_{2\text{A}}[\text{R}][\text{A}_0] \quad (13\text{a})$$

$$-(d[\text{Cu}^{\text{I}}\text{L}]/dt) = k_{\text{RP}}[\text{R}] \quad (13\text{b})$$

$$-(d[\text{Cu}^{\text{I}}\text{L}]/dt) = k_{2\text{B}}[\text{R}][\text{A}_0] \quad (13\text{c})$$

Equation 13a represents reaction via pathway A under conditions where R and P are fully equilibrated. However, if the rate of the oxidation step exceeds the rate of conversion of $\text{R} \rightarrow \text{P}$ ($k_{2\text{A}}[\text{A}_0] \gg k_{\text{RP}}$), eq 13b prevails and the reaction will become first order with respect to R (i.e., the conformational change becomes the rate-determining step). This situation may be encountered for many systems, in which significant conformational changes of the reagent of interest occur during the electron-transfer process, as the driving force and/or the self-exchange rate constant of the cross reagent are increased. As these latter parameters are increased even further, it is possible that $k_{2\text{B}}[\text{A}_0]$ may exceed k_{RP} , in which case the reaction will again become second order but will now be following pathway B (eq 13c). Corollary behavior will be observed for systems in which $K_{\text{PR}} \ll K_{\text{OQ}}^{-1}$.

On the basis of the current electrochemical investigation, we conclude that the copper complexes involving macrocyclic polythiaether ligands, which tend to favor planar coordination,³⁵ may all represent cases in which $K_{\text{PR}} \gg K_{\text{OQ}}^{-1}$ (i.e., P is more stable than Q). Thus, the reduction of the Cu(II)-polythiaether complexes may be proceeding by the intrinsically more favorable pathway A, while oxidations of the corresponding Cu(I) compounds proceed by pathway B whenever $k_{2\text{B}}[\text{A}_0] \gg k_{\text{RP}}$ —which appears to be the case in most of the systems studied.⁷ By contrast, the polypyridyl ligands, which tend to result in twisted coordination geometries with Cu(II),³⁸ may represent the case where $K_{\text{PR}} \ll K_{\text{OQ}}^{-1}$ (Q is more stable than P) such that the oxidations are proceeding by the more favorable pathway B while the reductions are forced to proceed by pathway A due to the sluggishness of the conformational change denoted by step k_{OQ} . This could account for the contrasting behavior of the self-exchange rate constants resolved from cross-reaction kinetic measurements for the copper complexes formed with the polythiaethers and with the polypyridyls as noted in the introduction.

Correlation to Other Copper(II)/(I) Systems. The foregoing behavior is consistent with several observations reported in the literature for electron-transfer reactions involving copper complexes. For example, in studying the reduction kinetics of a substituted phenanthroline complex, $\text{Cu}(\text{dpsmp})^{2-/3-}$, Lappin and co-workers³⁹ generally observed second-order kinetics consistent

with pathway B. With certain cross reagents, however, first-order behavior was observed corresponding to k_{OQ} as the rate-limiting step. Similar observations of both second- and first-order behavior have been reported for two blue copper proteins, i.e., for the reduction of rusticyanin⁴⁰ and for the oxidation of azurin.⁴¹ The assignment of this kinetic behavior to a dual pathway mechanism represented by our proposed square scheme is supported by spectral evidence indicating that two conformers of the copper binding site exist for both the oxidized and reduced forms of rusticyanin⁴⁰ and azurin.⁴²

Recently, Hoffman and Ratner⁴³ have expounded upon the importance of conformational changes in controlling gated electron transfer in biological systems. We propose that the square scheme, as outlined in this work, provides a ready explanation for such gated reactions involving copper enzymes.

Acknowledgment. We wish to acknowledge Wayne State University for providing a Rumble Graduate Fellowship to M.M.B. and the Getty Conservation Institute for a contract in support of a major portion of this research. The leaves of absence granted to M.M.B. by the University of Porto and the Instituto Nacional de Investigação Científica of Portugal are gratefully acknowledged. Appreciation is also expressed to Professor L. A. Ochrymowycz of the University of Wisconsin—Eau Claire for supplying the polythiaether ligands and to Professor R. L. Lintvedt of this department for the generous use of his electrochemical instrumentation.

Registry No. $\text{Cu}^{\text{II}}[14]\text{aneS}_4$, 57673-86-6; $\text{Cu}^{\text{I}}[14]\text{aneS}_4$, 93645-98-8; $\text{Cu}^{\text{II}}[14]\text{aneS}_4$ -diol, 117799-54-9; $\text{Cu}^{\text{I}}[14]\text{aneS}_4$ -diol, 87464-63-9; $\text{Cu}^{\text{II}}[15]\text{aneS}_4$, 57673-87-7; $\text{Cu}^{\text{I}}[15]\text{aneS}_4$, 87464-64-0; C, 7440-44-0; $\text{CH}_3\text{-OH}$, 67-56-1; HClO_4 , 7601-90-3.

Supplementary Material Available: Estimation of kinetic parameters plus figures giving additional cyclic voltammetric data and curves (6 pages). Ordering information is given on any current masthead page.

(39) Allan, A. E.; Lappin, A. G.; Laranjeira, M. C. M. *Inorg. Chem.* **1984**, *23*, 477-482. Cf.: Leupin, R.; Al-Shatti, N.; Sykes, A. G. *J. Chem. Soc., Dalton Trans.* **1982**, 927-930. The ligand denoted as dpsmp is 2,9-dimethyl-4,7-bis[(sulfonyloxy)phenyl]-1,10-phenanthroline.

(40) Lappin, A. G.; Lewis, C. A.; Ingledew, W. J. *Inorg. Chem.* **1985**, *24*, 1446-1450. When using the very strong reducing reagent Cr(II) for the reduction of rusticyanin, Lappin and co-workers observed uniquely different second-order kinetics than for other reagents exhibiting second-order behavior with this protein. If all reducing reagents were bound at the same active site on the protein, the Cr(II) results may represent reaction via pathway A while the reactions will all other reagents studied proceeded by pathway B.

(41) (a) Rosen, P.; Pecht, I. *Biochemistry* **1976**, *15*, 775-786. (b) Wilson, M. T.; Greenwood, C.; Brunori, M.; Antonini, E. *Biochem. J.* **1975**, *145*, 449-457. (c) Silvestrini, M. C.; Brunori, M.; Wilson, M. T.; Darley-Usmar, V. M. *J. Inorg. Biochem.* **1981**, *14*, 327-388.

(42) Szabo, A. G.; Stepanik, T. M.; Wayner, D. M.; Young, N. M. *Bio-phys. J.* **1983**, *41*, 233-244.

(43) Hoffman, B. M.; Ratner, M. A. *J. Am. Chem. Soc.* **1987**, *109*, 6237-6243.

(38) Burke, P. J.; Henrick, K.; McMillin, D. R. *Inorg. Chem.* **1982**, *21*, 1881-1886.